USING HiRISE DIGITAL ELEVATION MODELS TO INVESTIGATE THE PERIPHERAL PEAK RING MORPHOLOGY IN THE MARTIAN IMPACT CRATER TOOTING. J.C. Nycz and A.R. Hildebrand, Department of Geoscience, University of Calgary, 2500 University Drive Northwest, Calgary, Alberta, Canada. T2N 1N4. jcnycz@ucalgary.ca , ahildebr@ucalgary.ca

Introduction: Examination of MOC, MOLA HRSC, THEMIS, and most recently HiRISE data reveal the presence of partial or completely collapsed rims in some Martian impact craters. These collapse features have been named Peripheral Peak Rings (PPR) [1]. The 29km diameter impact crater Tooting is an excellent example of a young, largely uneroded complex impact crater which contains a PPR. By generating digital elevation models (DEM's) from HiRISE stereo data, detailed topographical information was obtained about the PPR in this crater. These data assisted in reconstructing the original rim of the Tooting crater before PPR formation, and allowed for the development of a robust PPR formation model.

Peripheral Peak Ring Formation: PPR are blocks from the crater rim that separated and slid downwards across the terraced zone until stopping near the crater floor. PPR form when the crater rim wall, after conventional slumping to form the terraced zone overlying the slump blocks (in the case of a complex crater), fails. PPR can be differentiated from the outermost terrace zone based on morphology. Whereas the slump blocks that form the terraces show downward displacement consistent with normal faulting, PPR undergo displacement that is mostly lateral, across the tops of the terraces (in the case of complex craters). This causes the tops of some PPR to be higher in elevation than the resulting crater rim, a phenomenon not seen in terraces. Examples of well developed PPR have been observed in simple craters as well, and most PPR have shapes that fit back into the depletion zone which once held them.

Impact Crater Tooting: The Tooting Impact crater is located at 23.4ºN, 207.5°E (Figure 1). Mouginis-Mark and Garbiel determined the age of Tooting to be between 0.4 and 1.7Myr [2]. Figure 1 shows the well developed monolithic PPR in the NW portion of the crater. Tooting has recently been almost completely covered by HiRISE stereo pairs which allow for the generation of Digital Elevation Models having sub meter resolution.

DEM Generation: DEM's were generated from stereo pairs having a maximum resolution of 25cm/pixel using stereo workstations and BAE's SOCET SET® photogrammetry software (see Acknowledgements). Using the USGS processing sequence, generated HiRISE DEM's were controlled to the MOLA DEM and groundtracks for absolute orientation. This results in an absolute error of the DEM's overall position in the X and Y direction of 50-100m. The absolute error in the Z direction for an entire DEM would be limited to the error in MOLA measurements, which in the case of steep topography, can be on the order of 10% of the elevation change within the 160m MOLA sample window (≈9m on a slope of 30°). [3].

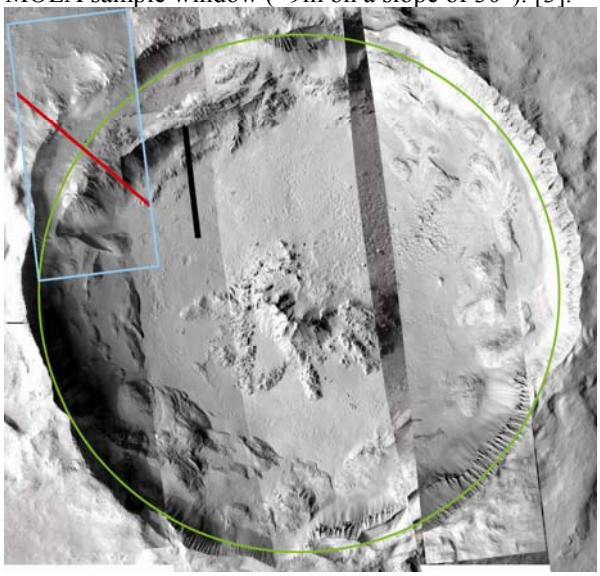

Figure 1. HiRISE mosaic of the 29km diameter crater Tooting. Green line is estimated position of crater rim immediately following the modification stage, blue box is area of DEM shown in Figure 2, and red line is location of topographic profile in Figure 3.

Of greater concern for this research is the relative vertical error within the DEM itself. Because HiRISE DEM's are derived from Photogrammatic methods as opposed to laser measurements, we calculate the expected vertical precision (EP) when describing the relative error within a DEM. EP is a function of image resolution, stereo viewing geometry and the RMS stereo matching error. Assuming a stereo matching error of 0.2 pixel, the expected precision (relative error) between two DEM posts based on HiRISE stereo geometry is approximately 0.25m. Stereo workstations used in the processing allow for any absolute errors within the DEM to be visually identified and manually corrected though a comprehensive editing process.

Rim Reconstruction: Figure 2 shows a portion of a DEM which covers the NW rim of Tooting. Reconstruction of the original rim of Tooting pre PPR formation was facilitated by using portions of the present rim that remain unslumped as inner "anchor" points. The ellipse denoting the original rim is seen in Figure 1

(green circle). Restored rim height was estimated based on extrapolation of the DEM, and MOLA heights of the unslumped rim around the crater as shown by [2]. Shape (i.e. slope) of the restored rim was based on MOLA profiles through the crater in places where no rim slumping post crater modification was evident.

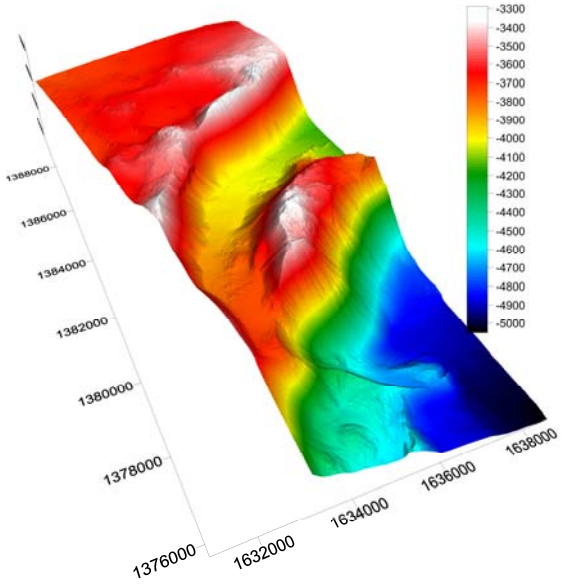

Figure 2. A portion of a DEM generated from HiRISE stereo pairs. Axis numbers correspond to northing, easting, and elevation (Mars 2000 datum). DEM shows the monolithic morphology of this PPR, and its relative height to the crater rim. See Figure 1 for location.

PPR Model: PPR formation and the resulting morphology can be categorized as a translational block slide. These are slides which involve translational motion (movement that involves changes in position as opposed to rotation) on a near planar, low angle slip surface. They are initiated when excavation undercuts or unloads the toe of an area of developed joints or planes (bedding or faults) which then act as weak layers, facilitating movement as discussed. Many concentric and radial faults are generated in crater rims during the cratering process, e.g. [4].

The Bindon Block slide of 1839 [5] is a well documented block slide whose characteristics are similar to what is seen in many Martian PPR. In this event, a single (500m by 400m by 140m) discrete block detached from the English coastline after strong marine erosion removed the toe of the landmass. The detached block remained intact through movement on a slide angle of 4.5°. In the general case of PPR development, whether a PPR stays intact after detachment (monolithic PPR) or breaks up into smaller blocks (rubbly PPR) depends on the cohesion of the block, the velocity of the slide, and therefore the amount of internal stress generated during sliding. In order for a formation model of PPR generation to be robust, the total unit volume of material must be conserved during all stages of the formation process. In addition, the separation, movement, and post PPR formation erosion of blocks must also be such that the final topographic profile (red profile in Figure 3) is achieved. Finally, the block movement must also allow for the palinspastic restoration of any layers seen outcropping in both the rim and the PPR. This process is shown in Figure 3.

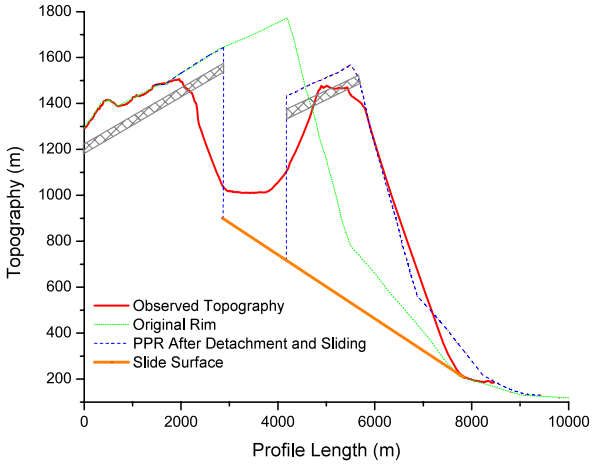

Figure 3. PPR Development. Location of observed topography is red line in Figure 1. After detaching at tension fracture and sliding along slip plane (angle is 7.9º), resulting rim and PPR have intermediate topography shown by dashed blue line. Subsequent settling of material reduces topography to that which is observed. Grey hatched layer corresponds to basalt layering seen in both the rim and PPR of Tooting. Elevation datum is -5000m. Vertical exaggeration is 4.3.

Slope Stability Modeling: The boundary conditions described above along with accurate layer thicknesses determined from the DEM allow for robust numerical modeling of the required strength distribution of subsurface layers. Using limit equilibrium methods and sensitivity analysis [6], restricted ranges for the strength of the ejecta, basalt, and rimrock seen in the exposed rim of the Tooting crater were obtained.

Acknowledgements: Topographic data described in this work were produced by using the Planetary Photogrammetry Guest Facility at the USGS Astrogeology Science Centre, established under the NASA Planetary Major Equipment Program and run under the NASA Planetary Geology and Geophysics (PG&G) Cartography Program. Techniques and software used to do the topomapping were developed by the USGS under funding from the PG&G program and MRO mission. We gratefully acknowledge the assistance of the USGS.

References: [1] Nycz and Hildebrand (2005), LPSC XXXVI Abstract #2167. [2] Mouginis-Mark and Garbeil (2007), *Meteoritics & Planet. Sci.*, 42, #9. [3] Zuber et al. (1992) *JGR* 97,E5. [4] Osinski & Spray (2005), *Meteoritics & Planet. Sci.*, 40, #12. [5] Dikau et al. (1996). "Landslide Recognition: *Identification, Movement and Causes*" John Wiley & Sons. [6] Hoek and Marinos (2007). *Soils and Rocks*, #2